

mixture stirred at room temperature for 1.5 h followed by flash chromatography; IR ν_{\max} 1775, 1600, 1515, 1345, 1250, 835, 730, 695 cm^{-1} ; UV λ_{\max} (cyclohexane) 236 (sh, 3.84), 242 (3.89), 248 (3.94), 357 (sh, 3.92), 362 (sh, 3.96), 370 (4.04), 380 (sh, 3.89), 394 nm (log ϵ 3.90); UV λ_{\max} (acetonitrile) 236 (3.86), 246 (3.85), 355 (sh, 3.83), 366 (3.90), 387 nm (log ϵ 3.73); ^1H NMR δ 6.16 (C_6D_6 , 6.21; CD_3CN , 6.12) (s, 1 H, $\text{CH}=\text{C}$), 6.8-7.8 (complex m, 9 H); ^{13}C NMR (Table II) δ 125.5 (d, C8/C10/C12), 128.6 (d, C9/C11), 138.6 (s, C7); mass spectrum (relative intensity), m/e (70 eV) 178 (100, M); exact mass calcd for $\text{C}_{14}\text{H}_{10}$ 178.078247, found 178.077960.⁴³

Subsequent fractions gave an unstable clear yellow oil proposed as **1-(hydroxyphenylmethyl)-1-(trimethylsilyl)cyclopropabenzene (31)**: 302 mg, 40%; ^1H NMR δ -0.29 (s, Me_3Si), 1.42 (s, OH), 5.09 (s, ArCH_2OH), 7.0-7.4 (complex m, 9 H); ^{13}C NMR δ -2.2 (q, Me_3Si), 44.6 (s, C1), 75.4 (d, ArCH_2OH), 115.4 and 115.8 (both d, C2/C5), 127.2, 127.9, 128.3, 128.5, and 128.7 (all d, aromatic CH), 130.9 and 131.8 (both s, C1a/C5a), 142.9 (s, phenyl); mass spectrum (relative intensity), m/e (18 eV) 268 (100, M).

(b) **29**: 166 mg, 33%, yielded after the mixture stirred at room temperature for 16 h; identical with the compound obtained in (a) above as the sole isolable product.

(iv) From **2** and *p*-Methoxybenzaldehyde. **1-((4-Methoxyphenyl)methylene)-1H-cyclopropabenzene (30)**: 181 mg, 31%, yellow crystalline solid; IR ν_{\max} 1780, 1600, 1510, 1300, 1250, 1030, 838, 735 cm^{-1} ; UV λ_{\max} (cyclohexane) 238 (sh, 3.88), 258 (3.94), 361 (sh, 3.93), 377 (4.09),

387 (sh, 3.95), 401 nm (log ϵ 4.00); UV λ_{\max} (acetonitrile) 257 (4.08), 356 (sh, 4.11), 372 (4.24), 393 nm (log ϵ 4.12); ^1H NMR δ 3.80 (s, OMe), 6.12 (C_6D_6 , 6.24; CD_3CN , 6.13) (s, 1 H, $\text{CH}=\text{C}$), 6.91 (d, J = 8.7 Hz, H8/H12), 7.08-7.47 (complex m, 4 H), 7.55 (d, J = 8.7 Hz, H9/H11); ^{13}C NMR (Table II) δ 55.4 (q, OMe), 114.4 (d, C9/C11), 126.6 (d, C8/C12), 158.1 (s, C10); mass spectrum (relative intensity), m/e (70 eV) 208 (100, M); exact mass calcd for $\text{C}_{15}\text{H}_{12}\text{O}$ 208.088 810, found 208.087 740.⁴³

Acknowledgment. Financial support from the NZ-US Educational foundation, Victoria University, the New Zealand Universities Grants Committee (for equipment grants), and the NSF (CHE 84-19099) in Utah is gratefully acknowledged.

Registry No. **2**, 4646-69-9; **7**, 493-04-9; **9**, 103322-14-1; **11**, 103322-15-2; **16**, 92012-56-1; **17**, 92012-57-2; **19**, 103322-16-3; **20**, 103322-17-4; **21**, 103322-18-5; **22**, 103322-19-6; **26**, 103322-20-9; **27**, 92012-54-9; **28**, 92012-55-0; **29**, 103322-21-0; **30**, 103322-22-1; **31**, 103322-23-2; $\text{Me}_2\text{C}=\text{CHOSO}_2\text{CF}_3$, 53282-30-7; $\text{Me}_2\text{C}=\text{C}(\text{SiMe}_3)\text{OSO}_2\text{CF}_3$, 73876-87-6; Me_3SiCl , 75-77-4; PhCOPh , 119-61-9; **18**, 92012-58-3; PhCOMe , 98-86-2; PhCOCF_3 , 434-45-7; PhCHO , 100-52-7; 4-MeOC₆H₄CHO, 123-11-5; Me_3CCHO , 630-19-3; 1,4-dihydronaphthalene, 612-17-9; naphthalene, 91-20-3; cyclopropa[*b*]naphthalene, 286-85-1.

Supplementary Material Available: Tables VI and VII listing thermal vibration parameters for non-hydrogen atoms and weighted mean planes (2 pages); tables of calculated and observed structure factors (7 pages). Ordering information is given on any current masthead page.

(43) As attempted recrystallization leads to decomposition, no melting point data are available; see text.

2,4,6-Tris(2,6-di-*tert*-butyl-4-substituted-phenoxy)-1,3,5,2,4,6-trioxatriphosphorinanes. Synthesis, Characterization, X-ray Structure, and Solid-State ^{31}P NMR of a Novel Family of Phosphorus(III)-Oxygen Heterocycles

D. W. Chasar,*[†] J. P. Fackler,[‡] A. M. Mazany,[†] R. A. Komoroski,^{†§} and W. J. Kroenke[†]

Contribution from the BF Goodrich Research & Development Center, Brecksville, Ohio 44141, and the Department of Chemistry, Texas A&M University, College Station, Texas 77843-3257. Received April 23, 1986

Abstract: The reaction of 2,6-di-*tert*-butylphenyl phosphorodichloridite or its para-substituted derivatives with 1 equiv of water in the presence of 2 equiv of trialkylamine forms a family of novel P(III)-O heterocycles, the 1,3,5,2,4,6-trioxatriphosphorinanes. These cyclic trianhydrides of substituted phosphorus acids are formed in 40-80% yields. The *p*-methyl derivative crystallizes in the $P\bar{1}$ space group of the triclinic crystal system with two molecules per unit cell (a = 10.896 (1) Å, b = 22.391 (3) Å, c = 9.785 (2) Å, α = 95.14 (1)°, β = 99.17 (1)°, and γ = 90.38 (1)°). The X-ray crystal structure of the *p*-methyl (and *p-tert*-butyl) derivative reveals that the P_3O_3 heterocycle exists in a distorted boat conformation with the three phosphorus atoms in nonequivalent environments. Two of the substituents are trans axial to one another while the third substituent is intermediate between axial and equatorial. The high-resolution solid-state ^{31}P NMR spectra confirm that each of the compounds examined in this study possesses three nonequivalent phosphorus atoms in the solid state. However, the ^{31}P NMR solution spectra of these compounds show that two of the phosphorus atoms are equivalent. This implies that the molecules each have a plane of symmetry in solution. While the compounds are stable to air or water, they melt with decomposition.

There has been a recent flurry of activity¹ in the isolation and characterization of novel trivalent phosphorus compounds **1** which owe their formation to sterically hindering ligand groups. For example, hindering groups prevent alternative reactions from occurring and effectively stabilize (protect) the labile P-P double bond² during the synthesis of **1**. We now report the synthesis and

characterization of a new class of trivalent phosphorus compounds **2** which also owe their stability to steric hindrance. These are formally cyclic anhydrides of monosubstituted phosphorous acids and belong to the tris(aryloxy)-1,3,5,2,4,6-trioxatriphosphorinane family.

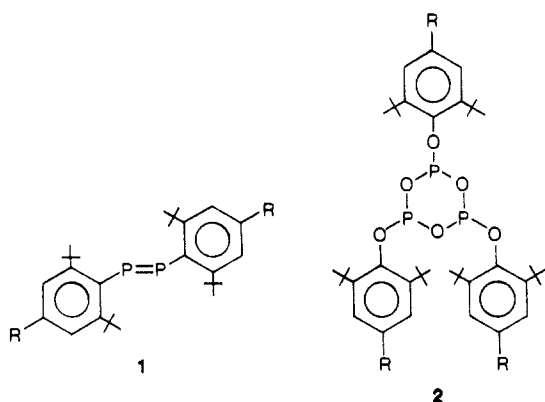
[†] BF Goodrich Co.

[‡] Texas A&M University.

[§] Current address: Department of Radiology, University of Arkansas for Medical Sciences, Little Rock, AR 72205.

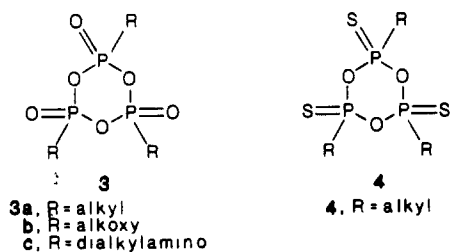
(1) Cowley, A. H. *Acc. Chem. Res.* **1984**, *17*, 386-392 and references cited therein.

(2) Smit, C. N.; van der Knaap, Th. A.; Bickelhaupt, F. *Tetrahedron Lett.* **1983**, *24*, 2031-2034.



- 2a, R = H
 b, R = CH₃
 c, R = CH₂CH₃
 d, R = Bu-*t*
 e, R = Bu-*n*
 f, R = OCH₃
 g, R = Bu-*sec*
 h, R = C(O)OCH₃
 i, R = C₆H₁₃
 j, R = CH₂CH₂C(O)OCH₂CH₃
 k, R = CH₂CH₂C(O)OCH₃

While the literature is replete with examples of similar six-membered rings of alternating phosphorus and oxygen atoms, most of these compounds possess *penta*valent phosphorus atoms as in 3a,^{3a} 3b,^{3b} 3c,^{3c} and 4⁴ and are often not well characterized.

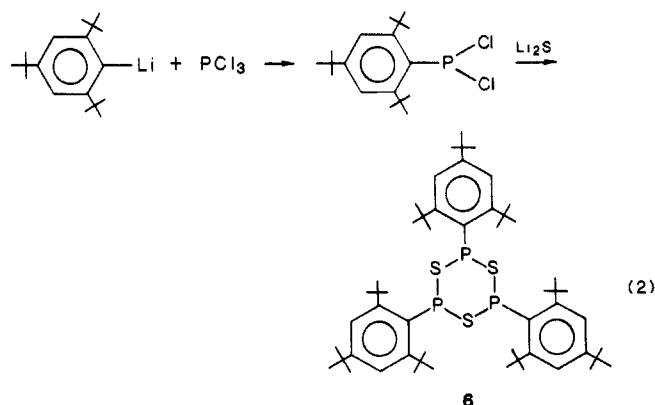
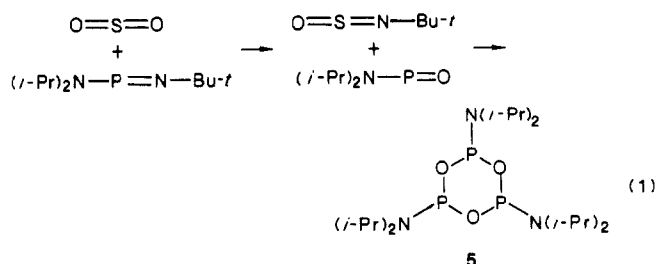


However, in 1980, Niecke et al.⁵ reported the synthesis (eq 1) and characterization (including a preliminary X-ray crystal structure) of 5, which is sensitive to both atmospheric moisture and air. In 1982, Cetinkaya et al.⁶ reported the synthesis (eq 2) and characterization, including the X-ray crystal structure, of a related trivalent phosphorus heterocycle 6, which also appears to owe its formation and stability to the sterically hindering ligand groups.

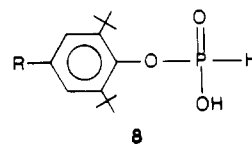
In this paper we report a simple yet novel synthesis and characterization of the family of compounds 2, an X-ray crystal structure of 2b (and 2d), and a correlation of the solid-state ³¹P NMR spectral characteristics to the X-ray structures.

Results and Discussion

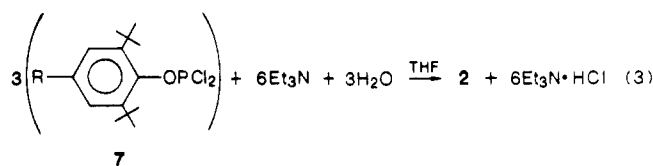
Synthesis and Characterization. The reaction of the dichloridite 7, which can be made by the reaction of the appropriate phenol with PCl₃ in the presence of a trialkylamine,⁷ with water results in its hydrolysis to the phosphorous acid 8.⁸ However, when 1



equiv of 7 and 2 equiv of triethylamine are first dissolved in tetrahydrofuran (THF) and 1 equiv of water (neat or in THF) is slowly added, 2 forms. 2 is isolated by filtering off the amine



hydrochloride and evaporating the THF. 2 is usually contaminated with 8, which can be removed with aqueous saturated sodium bicarbonate washes. Yields are typically 40–80%.



The elemental analyses of 2a–f corresponded to empirical formulas of RC₆H₂OPO. The IR spectra exhibited intense absorptions in the 930–960-cm⁻¹ range, which is consistent with P–O–P stretching frequencies.⁹ Even under field desorption/mass spectrometric (FD/MS) conditions where fragmentation can be kept to a minimum, parent ions are minor or nonexistent. In the ¹H NMR spectra (Table I), each proton-containing group gives rise to two absorptions in a 1:2 (upfield:downfield) ratio. Additionally, the ³¹P {¹H} NMR (CDCl₃) solution spectra of 2 exhibit two ³¹P absorptions, a triplet (*J* = 9–10 Hz) centered at ca. 127 ppm and a doublet at ca. 119 ppm, in a ratio of 1:2, respectively (Table VI). These data suggest two stereochemically different phosphorus atoms, two of one type and one of another, which in turn render their corresponding proton-containing substituents nonequivalent. These NMR characteristics are similar to those reported for 5⁵ and are consistent with the cyclic structure 2. The X-ray crystal structure, discussed below, confirms the structure of 2.

The products 2 are generally stable to air and moisture, particularly when they are free of acid 8. A water suspension of 2b or 2d maintained a pH of 7 for over 100 days. *tert*-Butyl hy-

(3) (a) Baer, E.; Sarma, G. R. *Can. J. Biochem.* **1967**, *45*, 1755–1761. (b) Kondo, H. Japanese Patent 49/55669, 1974; *Chem. Abstr.* **1974**, *81*, 151539f. Ogata, N.; Sanui, K.; Harada, M. *J. Polym. Sci., Polym. Chem. Ed.* **1979**, *17*, 2401–2411. (c) Cherepinski-Malov, V. D.; Gusev, A. I.; Nuretdinov, I. A.; Struchkov, Yu. T. *Zh. Strukt. Khim.* **1971**, *12*, 126–132; *Chem. Abstr.* **1971**, *75*, 11690z. Glonek, T.; Van Wazer, J. R.; Kleps, R. A.; Myers, T. C. *Inorg. Chem.* **1974**, *13*, 2337–2345.

(4) Keck, H.; Kuchen, W. *Phosphorus Sulfur* **1978**, *4*, 173–178. Maier, L.; *Phosphorus* **1975**, *5*, 253–259. Ecker, A.; Schmidt, U. *Monatsh. Chem.* **1972**, *103*, 736–743.

(5) Niecke, E.; Zorn, H.; Krebs, B.; Henkel, G. *Angew. Chem., Int. Ed. Engl.* **1980**, *19*, 709–710.

(6) Cetinkaya, B.; Hitchcock, P. B.; Lappert, M. F.; Thorne, A. J.; Goldwhite, H. *J. Chem. Soc., Chem. Commun.* **1982**, 691–693.

(7) Kujawa, F. M.; Shepard, A. F.; Dannels, B. F. U.S. Patent 3 271 481, 1966.

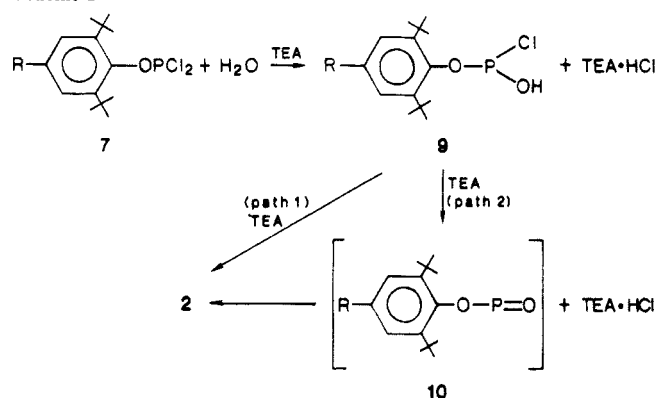
(8) Dannels, B. F.; Shepard, A. F. U.S. Patent 3 402 196, 1968.

(9) Rao, C. N. R. *Chemical Applications of Infrared Spectroscopy*; Academic: New York, 1963; p 294.

Table I. Summary of Physical Data on Compounds **2a-f**

compd	method	% yield ^a	mp, °C	IR (Nujol), cm ⁻¹	analyses			¹ H NMR (CDCl ₃), ppm ^b	
					C	H	P		
2a	1	58	115–132	932, 955	F ^d	66.36	8.46	12.23	1.36 (s, 18 H), 1.49 (s, 36 H), 7.02 (m, 3 H), 7.30 (m, 6 H)
					C ^d	66.65	8.39	12.28	
2b^c	2	75	184–186	930, 950	F	67.70	8.68	11.53	1.35 (s, 18 H), 1.47 (s, 36 H), 2.26 (s, 3 H), 2.29 (s, 6 H), 7.07 (s, 2 H), 7.11 (s, 4 H)
					C	67.65	8.71	11.63	
2c	1	48	149–155	930, 940	F	68.62	8.88	10.91	1.20 (t, <i>J</i> = 7.6, 3 H), 1.23 (t, <i>J</i> = 7.6, 6 H), 1.35 (s, 18 H), 1.48 (s, 36 H), 2.56 (q, <i>J</i> = 7.6, 2 H), 2.59 (q, <i>J</i> = 7.6, 4 H), 7.09 (s, 2 H), 7.13 (s, 4 H)
					C	68.53	8.99	11.05	
2d	2	80	212–220	950	F	69.83	9.45	10.00	1.28 (s, 9 H), 1.32 (s, 18 H), 1.35 (s, 18 H), 1.49 (s, 36 H), 7.29 (s, 2 H), 7.33 (s, 4 H)
					C	70.10	9.48	10.04	
2e	1	78	137–146	910, 920, 930, 945	F	70.17	9.44	9.75	0.93 and 0.94 (pair of t, <i>J</i> = 7.2, 9 H), 1.12–1.63 (m, 12 H), 1.34 (s, 18 H), 1.48 (s, 36 H), 2.51 and 2.55 (pair of t, <i>J</i> = 7.4, 6 H), 7.07 (s, 2 H), 7.11 (s, 4 H)
					C	70.10	9.48	10.04	
2f	1	67	140–150	948, 1060, 1170	F	63.82	8.21	10.97	1.36 (s, 18 H), 1.48 (s, 36 H), 3.76 (s, 3 H), 3.79 (s, 6 H), 6.83 (s, 2 H), 6.87 (s, 4 H)
					C	63.62	8.14	10.95	
2g-k^e	2		oils	940–945					

^a Isolated yield. ^b Downfield from internal (CH₃)₄Si. Coupling constants (*J*) are in hertz. ^c The ¹³C {¹H} NMR spectrum (CDCl₃) of **2b** exhibited a similar doubling effect of the ¹³C absorptions, with the exception of the *p*-methyl group (values are in ppm downfield from internal (CH₃)₄Si, and the more intense absorption is given first in each group): 21.17 (CH₃), 32.68 and 32.30 (C(CH₃)₃), 35.66 and 35.46 (C(CH₃)₃), 127.59 and 127.39 (C-3), 132.67 and 132.77 (C-4), 143.20 and 143.07 (C-2), 146.0 (d, *J*_{COP} = 5), and 147.0 (d, *J*_{COP} = 5, C-1). ^d F = found, C = calculated. ^e These oils were impure and impossible to purify. However, their ³¹P NMR (CDCl₃) solution spectra were consistent with those of **2a-f**, indicating the presence of the heterocyclic ring. Other phosphorus-containing impurities were present.

Scheme I

droperoxide does not oxidize **2b** to any appreciable extent at ambient temperature. However, **2** are thermally unstable and tend to decompose slowly during heating to their melting points, turning yellow to orange in color. This may explain the rather broad melting ranges for the compounds. However, rigorous purification of **2b** by using aqueous saturated sodium bicarbonate washes of a chloroform solution of **2b** and subsequent recrystallization of the resulting material from ethyl acetate or acetone did sharpen the melting point. Differential scanning calorimetry of **2b** or **2d**, including reheats, indicates that more than just melting occurs. A more detailed study of the chemistry of **2** will be discussed in a future publication.

At this time, two mechanisms for the formation of **2** are considered. It was shown that for each mole of **7** employed, 1 mol of water and 2 mol of triethylamine (TEA) afforded maximum yields. Less of either affords lower yields while more does not increase the yields. As water is added, **9** (Scheme I) undoubtedly forms. A similar reaction has been proposed¹⁰ for the reaction of phenyldichlorophosphine and water. The reaction of **9** with itself and triethylamine in a stepwise fashion (path 1) would afford **2**. On the other hand, TEA could promote the internal β -elimination of HCl from **9** to give **10**. **10** would be fleeting and could undergo a stepwise or concerted addition with itself to form **2**. There is precedent for a species like **10**. Both phosphinidenes **11** and phosphinidene oxides **12** have been proposed as intermediates in other reactions.¹¹ In fact, an aminophosphinidene oxide was

Table II. Crystal Data and Final Refinements for **2b**

mol formula	C ₄₅ H ₆₃ O ₆ P ₃
color	colorless
cryst dimens, mm	0.25 × 0.20 × 0.15
cryst class	triclinic
space group	P $\bar{1}$
cell dimens	
<i>a</i> , Å	10.896 (1)
<i>b</i> , Å	22.391 (3)
<i>c</i> , Å	9.785 (2)
α , deg	95.14 (1)
β , deg	99.17 (1)
γ , deg	90.38 (1)
molecules/cell	2
cell vol, Å ³	2346.8 (6)
density, g/cm ³	1.12
wavelength, Å	0.71073
<i>M_r</i>	792.91
linear abs coeff, cm ⁻¹	1.73
reflns with <i>F</i> > 3 σ (<i>F</i>)	3091
no. of parameters	487
final residuals	
<i>R</i>	0.046
<i>R_w</i>	0.056

proposed earlier⁵ (see eq 1). Work continues on the elucidation of the mechanism of formation of **2**.



2 was successfully prepared by two methods. If **7** is synthesized and purified in a separate step, then it can be converted to **2** by using triethylamine as base in THF as solvent. TEA·HCl precipitates and can be removed by filtration and **2** recovered from the filtrate by evaporation. However, it was found that the reaction of 1 mol of phenol with 1 mol of PCl₃ in 3 mol of tributylamine (purified) as solvent and base at 110 °C formed **7** in good yields. Addition of acetone, in which tributylamine hydrochloride is soluble, followed by a slow addition of 1 mol of water (in acetone) forms insoluble product **2**, which can be filtered off directly.

X-ray Crystal Structure of 2b. Table II summarizes the crystal data and final refinement of the structure. Tables III–V summarize the atomic positions of all atoms and the bond lengths and bond angles which involve the P and O atoms. The ORTEP drawing of the molecular structure of **2b** showing the 50% probability thermal ellipsoids is shown as Figure 1. The central feature is a puckered P₃O₃ ring which is best described as having a distorted boat conformation. The distortion results in the P₃O₃ ring being flattened and twisted relative to an ideal boat conformation. The three 2,6-di-*tert*-butyl-4-methylphenoxy exocyclic groups are

(10) Yoshifuji, M.; Nakayama, S.; Okazaki, R.; Inamoto, N. *J. Chem. Soc., Perkin Trans. 1* 1973, 2065–2068.

(11) Schmidt, U. *Angew. Chem., Int. Ed. Engl.* 1975, 14, 523–527.

Table III. Atom Positions for **2b**

atom	x/a	y/b	z/c
P(1)	0.7162 (2)	0.2474 (1)	0.9037 (2)
P(2)	0.4424 (2)	0.2488 (1)	0.8705 (2)
P(3)	0.5801 (2)	0.3660 (1)	0.9374 (2)
O(1)	0.6873 (4)	0.3159 (2)	0.9655 (4)
O(2)	0.5770 (4)	0.2310 (2)	0.8226 (4)
O(3)	0.4590 (4)	0.3208 (2)	0.8879 (4)
O(4)	0.7137 (4)	0.2147 (2)	1.0446 (4)
O(5)	0.3564 (4)	0.2435 (2)	0.7168 (4)
O(6)	0.5972 (4)	0.3853 (2)	0.7858 (4)
C(11)	0.7885 (6)	0.1132 (3)	1.0656 (6)
C(12)	0.8771 (7)	0.0754 (3)	1.1321 (7)
C(13)	0.9709 (7)	0.0983 (4)	1.2355 (8)
C(14)	0.9808 (7)	0.1590 (3)	1.2801 (8)
C(15)	0.8954 (6)	0.1990 (3)	1.2153 (7)
C(16)	0.8032 (6)	0.1755 (3)	1.1064 (7)
C(21)	0.3857 (5)	0.1569 (3)	0.5594 (6)
C(22)	0.3769 (6)	0.0950 (3)	0.5319 (7)
C(23)	0.3063 (6)	0.0607 (3)	0.6053 (7)
C(24)	0.2340 (6)	0.0890 (3)	0.6957 (6)
C(25)	0.2405 (6)	0.1516 (3)	0.7265 (6)
C(26)	0.3258 (6)	0.1838 (3)	0.6647 (6)
C(31)	0.7428 (6)	0.4666 (3)	0.7725 (6)
C(32)	0.7654 (7)	0.5284 (3)	0.7796 (7)
C(33)	0.6664 (8)	0.5681 (3)	0.7776 (7)
C(34)	0.5445 (7)	0.5475 (3)	0.7567 (6)
C(35)	0.5165 (6)	0.4851 (3)	0.7492 (6)
C(36)	0.6189 (6)	0.4468 (3)	0.7692 (6)
C(1A)	0.6808 (6)	0.0840 (3)	0.9592 (7)
C(1B)	0.6783 (7)	0.0152 (3)	0.9580 (8)
C(1C)	0.6950 (7)	0.0968 (3)	0.8105 (8)
C(1D)	0.5528 (7)	0.1046 (3)	0.9934 (8)
C(1E)	1.0628 (9)	0.0555 (4)	1.3047 (10)
C(1F)	0.9090 (7)	0.2661 (3)	1.2657 (7)
C(1G)	0.9636 (7)	0.2997 (3)	1.1578 (7)
C(1H)	1.0060 (8)	0.2767 (3)	1.4035 (8)
C(1J)	0.7878 (7)	0.2933 (3)	1.2984 (7)
C(2A)	0.1438 (6)	0.1786 (3)	0.8154 (7)
C(2B)	0.1295 (7)	0.2468 (3)	0.8192 (7)
C(2C)	0.1772 (9)	0.1603 (3)	0.9616 (8)
C(2D)	0.0139 (7)	0.1535 (4)	0.7454 (10)
C(2E)	0.3018 (8)	-0.0067 (3)	0.5796 (8)
C(2F)	0.4568 (7)	0.1915 (3)	0.4625 (7)
C(2G)	0.3913 (10)	0.1749 (4)	0.3140 (8)
C(2H)	0.4619 (8)	0.2599 (4)	0.4879 (8)
C(2J)	0.5934 (8)	0.1715 (3)	0.4788 (9)
C(3A)	0.3793 (6)	0.4648 (3)	0.7192 (7)
C(3B)	0.3307 (6)	0.4567 (3)	0.8537 (7)
C(3C)	0.3586 (6)	0.4084 (3)	0.6188 (7)
C(3D)	0.3004 (7)	0.5138 (3)	0.6454 (8)
C(3E)	0.6939 (8)	0.6350 (3)	0.7930 (8)
C(3F)	0.8546 (6)	0.4252 (3)	0.7680 (8)
C(3G)	0.8206 (7)	0.3652 (4)	0.6793 (8)
C(3H)	0.9136 (7)	0.4120 (3)	0.9162 (8)
C(3J)	0.9576 (7)	0.4558 (4)	0.7017 (9)

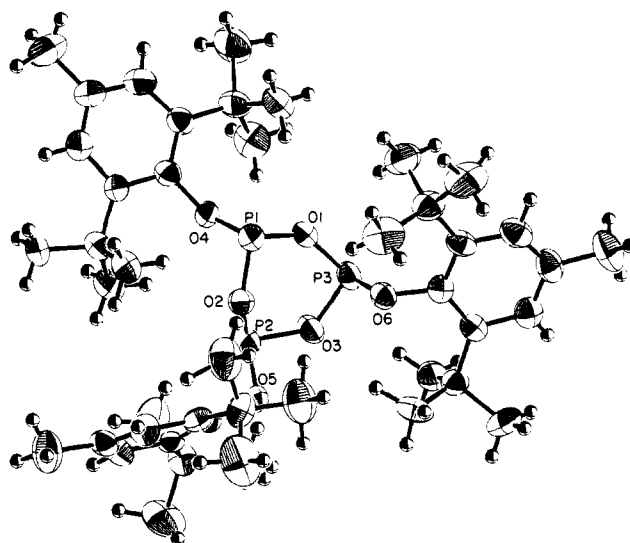
Table IV. Selected Bond Distances (Å) for **2b**

P(1)-O(2)	1.619 (4)	P(3)-O(6)	1.621 (4)
P(1)-O(4)	1.622 (4)	P(3)-O(1)	1.632 (4)
P(1)-O(1)	1.649 (4)	P(3)-O(3)	1.640 (4)
P(2)-O(3)	1.613 (4)	O(4)-C(16)	1.416 (7)
P(2)-O(5)	1.635 (4)	O(5)-C(26)	1.405 (6)
P(2)-O(2)	1.651 (4)	O(6)-C(36)	1.421 (6)

Table V. Selected Bond Angles (deg) for **2b**

O(2)-P(1)-O(4)	100.2 (2)	O(1)-P(3)-O(3)	99.0 (2)
O(2)-P(1)-O(1)	96.8 (2)	P(3)-O(1)-P(1)	138.3 (3)
O(4)-P(1)-O(1)	97.7 (2)	P(1)-O(2)-P(2)	128.9 (2)
O(3)-P(2)-O(5)	96.9 (2)	P(2)-O(3)-P(3)	132.9 (3)
O(3)-P(2)-O(2)	99.2 (2)	C(16)-O(4)-P(1)	127.3 (4)
O(5)-P(2)-O(2)	98.5 (2)	C(26)-O(5)-P(2)	112.7 (3)
O(6)-P(3)-O(1)	102.4 (2)	C(36)-O(6)-P(3)	119.4 (3)
O(6)-P(3)-O(3)	98.1 (2)		

identified by their connectivity to the P_3O_3 ring as P(1)/O(4), P(2)/O(5), and P(3)/O(6). Two of the three phenoxy groups

Figure 1. Molecular structure of **2b** (50% probability thermal ellipsoids).

are located in axial positions, P(3)/O(6) above and P(1)/O(4) below a reference plane consisting of the three ring P atoms. Because of the distortion from an ideal boat conformation, the assignment of P(2)/O(5), the third phenoxy group, to either an axial or an equatorial position is more complicated. However, on the basis of the results of the ^{31}P NMR studies presented in the next section, the P(2)/O(5) phenoxy group, which extends above the P(1)-P(2)-P(3) reference plane, is assigned to an axial position.

Figure 1 and the data in Tables III-V clearly show that the **2b** molecule is asymmetric in the solid state, with each of the three ring P atoms situated in different local environments. The solid-state ^{31}P NMR results (see next section) confirm that the P atoms are nonequivalent. However, a small rotation of O(5) in the solid-state conformation (Figure 1) toward the center of the P_3O_3 ring is sufficient to create a mirror plane. After such a rotation, P(2)/O(5) clearly occupies an axial position as per our assignment. Based on the solid-state molecular structure, no simple rotation pattern is able to provide a chair conformation with a mirror plane of symmetry.

The packing pattern of **2b** molecules in the crystal was investigated in an attempt to understand the origin of the solid-state distortion of the P_3O_3 boat. No obvious intermolecular interactions were found. The conclusion is that the distortion probably is caused by intramolecular effects resulting from the sterically hindering phenoxy groups, with, perhaps, some influence from crystal-lattice forces.

Although it will not be discussed in detail, the X-ray crystal structure of **2d** has been determined to a final R_w value of about 10%. The conformations of the P_3O_3 ring and the P_3O_6 fragment are virtually indistinguishable from their counterparts in **2b**. This result is expected, since their molecular configurations are very similar.

The X-ray crystal structure of only one other heterocyclic compound containing the P_3O_3 ring has been reported in the literature.⁵ It is essentially **2b** with the exocyclic trisubstituted phenoxy groups replaced with the less bulky, but still sterically hindering, diisopropylamino groups. This structure also is best described in terms of a distorted boat conformation for the P_3O_3 ring. Unfortunately, only a preliminary structure determination has been reported, because the structure is disordered, with 23% of the molecules having a different orientation but very probably with the same conformation as the other 77%.¹² Using the atom positions supplied by Krebs,¹² we verified that the P_3O_3 ring has a boat conformation in the solid state. In this case the distortion from an ideal boat conformation is relatively small compared to **2b**. It is noteworthy that the three amino groups occupy equatorial

(12) Krebs, B., private communication, March 2, 1983.

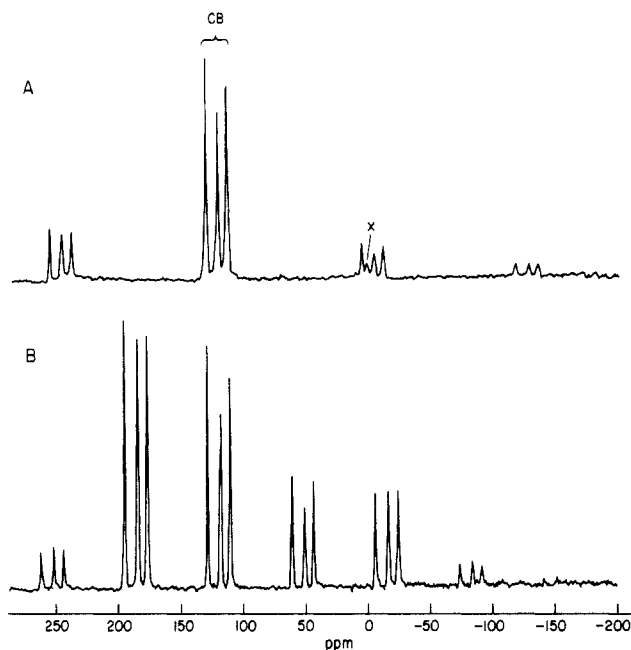


Figure 2. ^{31}P CPMAS spectrum of compound **2d** at two spinning speeds: (A) at 4.49 kHz and (B) at 2.42 kHz. The centerbands are denoted CB. An impurity is denoted by X.

positions, not axial positions as for **2b**.

The crystal structure of a heterocyclic compound closely related to **2d** has been reported in the literature.⁶ It has a P_3S_3 central ring, but in place of the exocyclic 2,4,6-tri-*tert*-butylphenoxy groups in **2d** there are three exocyclic 2,4,6-tri-*tert*-butylphenyl groups. In contrast to **2d** and **2b**, the P_3S_3 analogue has the *chair* conformation with the exocyclic groups in the equatorial positions. Also, compared to the P_3O_3 rings in **2d** and **2b**, the P_3S_3 ring exhibits little deviation from an ideal chair conformation. We speculate that the increased size of the P_3S_3 ring helps to eliminate intramolecular interactions between the three tri-*tert*-butylphenyl groups. In contrast, the smaller P_3O_3 ring in **2d** is sterically influenced by the tri-*tert*-butylphenoxy groups to assume the observed, highly distorted boat conformation. Consistent with the premise that steric effects from the bulky substituted aromatic groups cause the observed distortions from an ideal boat conformation for **2b** and **2d** is the fact that when the tri-*tert*-butylphenoxy groups in **2d** are replaced by less bulky diisopropylamino groups,⁵ the distortion of the P_3O_3 ring from an ideal boat conformation is significantly decreased.

The prototype molecule for the existence of stabilized P_3O_3 heterocyclic ring compounds containing only P(III) is P_4O_6 , which has an adamantane-like cage structure.¹³ However, it also can be considered as a P_3O_3 ring in a chair conformation which is capped (and stabilized) by a PO_3 group. Although the POP angles in **2b** (Table V) are significantly larger than the mean POP angle in P_4O_6 (127.0°), the mean P–O bond length (1.634 Å) and the mean OPO angle (98.7°) compare favorably with their counterparts in P_4O_6 (1.656 Å and 99.5°). These comparisons strengthen our contention that in the trioxatriphosphorinane compounds; the P_3O_3 ring is stabilized by steric effects from the exocyclic 2,6-di-*tert*-butyl-4-substituted-phenoxy groups.

Solid-State ^{31}P NMR. Figure 2 shows the full cross-polarization/magic angle spinning (CPMAS) spectrum of compound **2d** at two spinning speeds. The general features of the spectrum in Figure 2 are found in the solid-state spectra of all the compounds studied here. In the solid-state spectrum, MAS sidebands are seen when the rate of sample spinning is less than about half the width of the chemical shift anisotropy (CSA) powder pattern.¹⁴ The

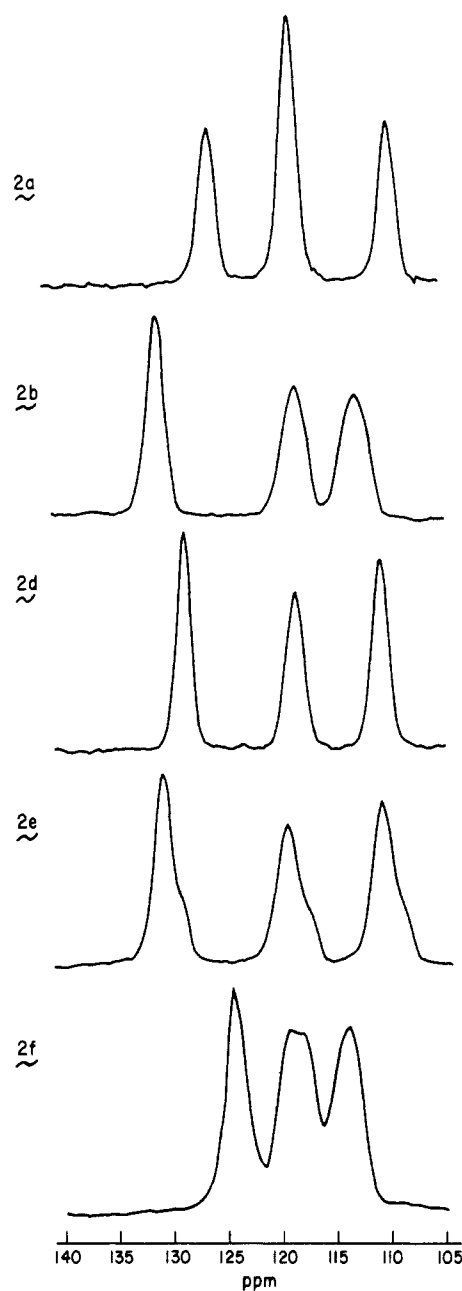


Figure 3. Centerband patterns of the ^{31}P CPMAS spectra of some trioxatriphosphorinanes.

centerband or isotropic chemical shift can be identified by the fact that it does not change position with a change in MAS speed. The CSAs of the phosphorus atoms in the compounds studied here are about 450 ppm, judging from the extent of the sideband patterns. We made no attempt to determine exact CSA patterns by mapping out the sideband behavior as a function of spinning speed.¹⁵ Minor variations in relative intensity among the three peaks throughout the sideband pattern were seen.

Figure 3 shows the centerband patterns of the ^{31}P solid-state spectra of five of the compounds prepared here. For the most part, all consist of three single peaks with line widths ranging from 55 to 125 Hz. Even with computer-resolution enhancement and precise adjustment of the magic angle, we were never able to resolve splittings from $^2J_{\text{PP}}$ ($\sim 9\text{--}10$ Hz), as seen in the solution spectra. In addition, with the possible exception of the center line for compound **2f**, we saw no evidence for ^{31}P homonuclear dipolar coupling in any of the solid-state spectra. When significant homonuclear dipolar coupling is present in addition to the CSA, a complicated manifold is seen instead of a single, relatively narrow

(13) Jansen, M.; Voss, M.; Deiseroth, H.-J. *Angew. Chem., Int. Ed. Engl.* **1981**, *20*, 965.

(14) Fyfe, C. A. *Solid State NMR for Chemists*; C.F.C.: Guelph, Canada, 1984.

(15) Herzfeld, J.; Berger, A. E. *J. Chem. Phys.* **1980**, *73*, 6021–6030.

Table VI. Solution (CDCl₃) and Solid-State ³¹P NMR Chemical Shifts

compd	δ , ppm ^{a,b}		
	1 ^c	2 ^d	3
2a , soln	127.5	119.7	
2a , solid	126 (0.57)	119 (1.00)	110 (0.57)
2b , soln	127.9	120.0	
2b , solid	132 (1.00)	119 (0.86)	114 (0.91)
2d , soln	128.1	119.4	
2d , solid	129 (0.94)	119 (0.89)	111 (1.00)
2e , soln	127.8	119.6	
2e , solid	131 (1.00)	120 (0.90)	111 (0.99)
2f , soln	128.3	120.3	
2f , solid	124 (0.85)	119 ^e (1.00)	114 (0.80)

^aRelative to external 85% aqueous H₃PO₄. ^bRelative intensities in parentheses. ^cA one-phosphorus triplet in solution. ²J_{PP} = 10 Hz, except for **2e**, where ²J_{PP} = 9 Hz. ^dA two-phosphorus doublet in solution. ²J_{PP} = 10 Hz, except for **2e**, where ²J_{PP} = 9 Hz. ^eAverage of double maximum.

peak.¹⁶ For compound **2b**, where the ³¹P–³¹P distance is 2.95 Å, a dipolar coupling of about 1150 Hz is predicted. Apparently, this is sufficiently less than the MAS speed so that no effect of homonuclear dipolar coupling is seen in the spectrum.

The isotropic ³¹P chemical shifts (and relative intensities) in the solid are compared to the corresponding chemical shifts in solution in Table VI. With the exception of compound **2a**, the three lines in each of the centerbands are approximately equal in intensity. For compound **2a**, each of the outer lines is only 57% the intensity of the inner line. We attribute this discrepancy, and the minor variations seen for some of the other compounds, to variations in the spread of total intensity across the sideband patterns and possibly to differences in the CP rate among the three lines.

The observation of three, well-resolved peaks for each of the compounds in Table VI and Figure 3 indicates that the three phosphorus atoms are in significantly different environments in the crystal lattice. This is unlike the behavior in solution, where two of the phosphorus atoms are equivalent. Comparison of the solution and solid-state results shows that the downfield and center lines of the solid-state spectra correspond to the chemical shifts seen in solution. In particular, the chemical shift of the center line (doublet in solution) is constant among the compounds studied in solution or in the solid state. The upfield line in the solid-state spectra is unique to the solid state, and we assume that it corresponds to the other phosphorus atom occurring at 119–120 ppm in solution.

The single-crystal X-ray studies of compounds **2b** and **2d** indicate that the P₃O₃ ring exists in a distorted boat conformation with the phenoxy groups oriented as discussed above. We interpret the X-ray and ³¹P NMR results in the following way. In solution, the heterocyclic ring exists primarily in a boat conformation, rendering the P(2) and P(3) phosphorus atoms with cis axial substituents equivalent (120 ppm) since a plane of symmetry containing O(3)–P(1)–O(4) (Figure 1) exists. The heterocyclic ring is in the same conformation for all the compounds in solution. In the solid state, all of the compounds have approximately the same distorted boat conformation as compounds **2b** and **2d**, giving rise to similar three-line ³¹P spectra. Minor differences in chemical shifts among the compounds arise from small differences in ring conformation in the solid state, small differences in substituent orientation in the crystal, or other crystal-packing effects. In the above interpretation, the peak at 124–132 ppm is assigned to the phosphorus atom P(1) with a trans axial substituent, the peak at 119–120 ppm to the phosphorus atom P(3) with an axial substituent, and the peak at 110–114 ppm to the phosphorus atom P(2) with the substituent somewhat displaced from an axial orientation.

The above interpretation is by no means the only one possible. The assignments of the boat conformation in solution rest on the

X-ray results and the coincidence of the solution and solid-state ³¹P chemical shifts. This may be coincidental, and the heterocyclic ring may adopt one or more different conformations in solution. Some ambiguity also exists regarding the solid-state ³¹P NMR assignments, since the difference in chemical shift between two adjacent peaks is typically on the order of 5–10 ppm. Such a difference is small enough to be attributable in large part to crystal-packing effects, masking differences due to changes in ring conformation.

Solid-state ³¹P NMR spectra were also obtained for impure preparations of compounds **2g** and **2h**. The general features of these spectra were the same as those described for the other compounds, except that additional, unidentified peaks were seen in the 100–140 ppm region.

Experimental Section

Melting points were obtained on a Mel-Temp apparatus and are uncorrected. Elemental analyses were performed at Huffman Labs, Wheatridge, CO. Infrared spectra were obtained on a Perkin-Elmer Model 467 spectrometer. All field desorption and FAB mass spectra were obtained on a Finnigan MAT 311A mass spectrometer. All ¹H NMR spectra were obtained on a Bruker WH-200 instrument, and the chemical shifts are reported in parts per million (ppm) from internal (CH₃)₄Si.

High-resolution, solid-state ³¹P NMR spectra were acquired at 36.44 MHz by using cross-polarization/magic angle spinning (CPMAS) and dipolar decoupling on a Bruker HX90E/SXP spectrometer retrofitted with a BDR-90C unit. The Bruker solids ¹³C NMR probe was modified for operation in the approximate range of 32–37 MHz. The powdered samples were tightly packed in 9-mm-o.d. Delrin rotors of the Andrew geometry. The spinning angle was adjusted to the magic angle by acquiring several spectra and determining the value with the minimum line width. Magic angle spinning was generally performed at 2.2–2.4 kHz, although several spectra were obtained at about 4.5 kHz. Typical conditions were as follows: recycle time, 2 s; P–H contact time, 1 ms; data acquisition time, 50 ms; 90° radio frequency pulse width, 4.8 μs; spectral width, 20 kHz; and number of transients, 50–3000. Approximate chemical shifts were measured relative to the spectrometer frequency, which previously had been calibrated relative to a separate sample of 85% aqueous H₃PO₄.

The proton-decoupled ³¹P spectra in solution were acquired on the same instrument as above using the standard multinuclear probehead. Samples were run with CDCl₃ as solvent in 10-mm tubes. Chemical shifts were measured relative to an external capillary of 85% aqueous H₃PO₄. Typical conditions were as follows: recycle time, 10 s; 90° radio frequency pulse width, 15 μs; spectral width, 12048 Hz in 8192 points.

The X-ray intensity data (13380 reflections; 3.0° ≤ 2θ ≤ 60.0°; *h*, ±*k*, ±*l*; ω scan) from a single crystal of **2b** were recorded on a Nicolet P3F four-circle diffractometer at ambient temperature using graphite-monochromated Mo K_α radiation. The 3091 reflections with *I* > 3.0σ(*I*) were corrected for Lorentz, decay, polarization, and absorption effects and used to solve the structure. The initial P and O atom positions were located by using the direct-methods routine SOLV of the SHELXTL crystallographic computation package. All remaining non-hydrogen atom positions were located by subsequent difference Fourier techniques. Final least-squares refinements were made by using the UCLA Crystallographic Package installed on a DEC VAX-750.

The X-ray crystal structure of **2d** also was determined by following the general procedure outlined above.

General Synthetic Procedure. Method 1. Water (0.30 g, 0.017 mol) is added to a cooled (0–5 °C) stirred solution of 2,4,6-tri-*tert*-butylphenyl phosphorodichloridite⁷ (6.0 g, 0.017 mol) and triethylamine (3.34 g, 0.033 mol) in dry tetrahydrofuran (100 mL). This is stirred at 0–5 °C for 0.5 h. The mixture is filtered and the filtrate evaporated to dryness to afford a white glass. After this glass is stirred in an aqueous saturated NaHCO₃ solution for 10 min, it is filtered, washed with water, and air dried. This glass can be crystallized by stirring it in acetonitrile.

Method 2. 2,6-Di-*tert*-butyl-4-methylphenol (500 g, 2.27 mol) and tributylamine (1262 g, 6.81 mol, Eastman purified) are charged into a 5-L round-bottom flask equipped with an overhead stirrer, thermometer, dropping funnel, water condenser, and nitrogen inlet. Phosphorus trichloride (311.8 g, 2.27 mol) is added dropwise with stirring, followed by heating at 110 °C for 1 h. The mixture is cooled to room temperature, acetone (1150 mL) is added, and water (40.8 g, 2.27 mol) in acetone (100 mL) is added dropwise over 45 min. Stirring is continued for 0.5 h. The slurry is filtered and the resulting solid washed with acetone and air dried to afford 479.5 g (79%) of product, mp 173–183 °C.

An analytical sample is prepared by washing a chloroform solution of **2b** with aqueous saturated NaHCO₃ (2×) and water (1×), evaporating

the chloroform, and recrystallizing the glass from acetone, which affords white crystals, mp 184–186 °C.

Acknowledgment. We thank Perry Matheny for carrying out the synthetic work and Prof. Leo Paquette for helpful discussions. A.M.M. thanks the Robert A. Welch Foundation for a fellowship, and J.P.F. thanks the National Science Foundation (NSR 84-

01414) and the Welch Foundation for partial support.

Supplementary Material Available: Tables S1 and S2 listing hydrogen atomic parameters and anisotropic thermal parameters (2 pages); tables of observed and calculated structure factor amplitudes for **2b** (14 pages). Ordering information is given on any current masthead page.

Intramolecular Nucleophilic Catalysis during Alkaline Hydrolysis of Nonenolizable β -Keto Esters

William N. Washburn* and Ewell R. Cook

Contribution from the Life Sciences Division, Eastman Kodak Company, Rochester, New York 14650. Received November 25, 1985

Abstract: Kinetic and ^{18}O -labeling studies demonstrate that in the hydrolysis of nonenolizable acetoacetate esters, the carbonyl hydrate acts as a nucleophilic catalyst. A cyclic four-membered lactone is formed and later opens. Structure/reactivity studies showed the rate-determining step to be a function of the $\text{p}K_{\text{a}}$ of the leaving group and the substituent bound to C_3 of the acetoacetate residue. Rate accelerations of 4 to 10^4 were observed for hydrolyses of the corresponding *p*-nitrophenyl esters, depending on the substituent at C_3 .

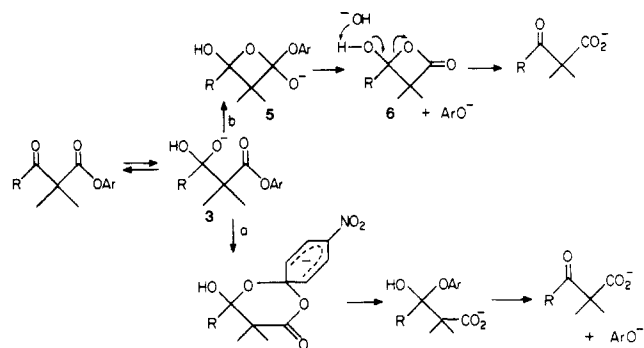
The intramolecular catalysis of alkaline hydrolysis of carboxylic esters due to a neighboring γ - or δ -hydroxyl group has been well documented.¹ Rate accelerations have also been reported for γ -keto esters since the hydrates of the carbonyls act as internal nucleophiles.² Hydrolytic rate enhancements of 10^4 for *o*-acetoxybenzaldehyde^{2k} and 10^5 for methyl *o*-formylbenzoate^{2c} have been reported. Our investigation of the hydrolysis of nonenolizable β -keto esters demonstrates that substantial acceleration arises from the β -carbonyl.

Esters **1a–g** were prepared to evaluate the effect of a β -carbonyl during hydrolysis of sterically congested esters. The hydrolyses of **1a–g** were followed by ^1H NMR at pH 12 in 1:1 $\text{CD}_3\text{CN}/\text{H}_2\text{O}$. The initial hydrolysis products for each ester, except for **1g**, were *p*-nitrophenoxide and the corresponding substituted acetoacetate ion, which, depending on the substituent at C_4 , decarboxylated. Alkaline hydrolysis of **1g** yielded chloroform and the half ester of *p*-nitrophenyl dimethylmalonate. By ^1H NMR, **1e** and **1f** were extensively hydrated; the ratios of hydrate to ketone were 1:3 and 3:1, respectively, in 1:1 $\text{CD}_3\text{CN}/\text{D}_2\text{O}$.

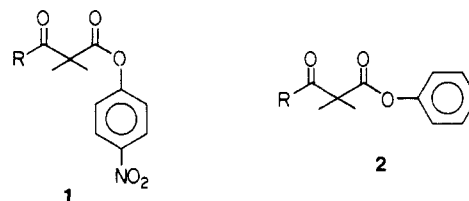
The hydrolysis rates of **1a–e**, measured at 400 and 290 nm, respectively, in 1:1 $\text{CH}_3\text{CN}/\text{aqueous potassium phosphate buffer}$ (0.15 μm) over a pH range of 10–13.3, were first order in hydroxide ion. The hydrolysis rate of **1f** was first order in hydroxide ion up to pH 11 but became pH independent above pH 13, which suggests that the kinetically active species was the hydrate anion **3**, which for **1f** was almost completely formed at pH 13.

For hydrolysis of **1a–e** at pH 13.3, a plot of $\log k$ vs. σ^* (Figure 1) showed $\rho^* = 1.7$. Since the $\sigma^*\rho^*$ plot for the hydrolysis of *p*-nitrophenyl α -substituted isobutyrate esters under identical conditions gave $\rho^* = 0.3$, it was apparent that the insertion of

Scheme I



the carbonyl group between the substituent *R* and the α -carbon greatly increased the rate response to *R*. If the kinetically active species were the ionized ketone hydrate **3**, the observed $\rho^* = 1.7$ would be in accord with the reported $\rho^* = 1.7$ for carbonyl hydration and 1.4 for ionization of the corresponding hydrate in H_2O .^{3,4}



- | | |
|--|--|
| a R = CH_3 | a R = CH_3 |
| b R = CH_2OMe | b R = CH_2OMe |
| c R = $\text{CH}_2\text{OC}_6\text{H}_5$ | c R = $\text{CH}_2\text{OC}_6\text{H}_5$ |
| d R = CH_2Cl | d R = CH_2Cl |
| e R = CHF_2 | e R = CHF_2 |
| f R = CF_3 | f R = CF_3 |
| g R = CCl_3 | |

In the course of elucidating the reaction mechanism, the corresponding phenyl ester series **2a–f** was prepared. The nonlinearity

(3) Greenzaid, P.; Luz, Z.; Samuel, D. *J. Am. Chem. Soc.* **1967**, *89*, 749.
(4) Bell, R. P. *Adv. Phys. Org. Chem.* **1966**, *4*, 1.

(1) Kirby, A. J. *Adv. Phys. Org. Chem.* **1980**, *17*, 183.
(2) (a) Bhatt, M. V.; Rao, G. V.; Rao, K. S. *J. Org. Chem.* **1979**, *44*, 984.
(b) Walder, J. A.; Johnson, R. S.; Klotz, I. M. *J. Am. Chem. Soc.* **1978**, *100*, 5156. (c) Bender, M. L.; Silver, M. S. *J. Am. Chem. Soc.* **1962**, *84*, 4589.
(d) Bender, M. L.; Reinstein, J. A.; Silver, M. S.; Mikulak, R. *J. Am. Chem. Soc.* **1965**, *87*, 4545. (e) Newman, M. S.; Hishida, S. *J. Am. Chem. Soc.* **1962**, *84*, 3582. (f) Shalitin, Y.; Bernhard, S. A. *J. Am. Chem. Soc.* **1964**, *86*, 2292. (g) Ramirez, F.; Hansen, B.; Desai, N. B. *J. Chem. Soc.* **1962**, *84*, 4588. (h) Burrows, H. D.; Topping, R. M. *J. Chem. Soc., Perkin Trans. 2* **1975**, 571. (i) Bowden, K.; Last, A. M. *J. Chem. Soc., Perkin Trans. 2* **1973**, 345. (j) Bowden, K.; Last, A. M. *J. Chem. Soc., Perkin Trans. 2* **1973**, 351. (k) Holleck, L.; Melkonian, G. A.; Rao, S. B. *Naturwissenschaften* **1958**, *45*, 438.